

Stress evolution in NiCoFeCrMn and NiCoFeCr high-entropy alloys irradiated by helium and krypton ions

M.M. Belov^{1,}, I.A. Ivanov^{2,3}, V.V. Uglov¹, S.V. Zlotski¹, K. Jin⁴, N.A. Stepanjuk¹, A.E. Ryskulov², A.L. Kozlovskiy^{2,3}, M.V. Koloberdin^{2,3}, A.E. Kurakhmedov², A.D. Sapar²*

¹*Belarusian State University, Minsk, Belarus*

²*Institute of Nuclear Physics, Nur-Sultan, Kazakhstan*

³*L.N. Gumilyov Eurasian National University, Nur-sultan, Kazakhstan*

⁴*Beijing Institute of Technology, Beijing, China*

**mb17023@gmail.com*

Abstract. The paper presents the results of coarse-grained (80 and 100 μm) bulk high-entropy alloys CoCrFeNi and CoCrFeMnNi samples with X-ray diffraction method in non-irradiated and ion irradiated states (He^{2+} , 40 keV, $2 \times 10^{17} \text{ cm}^{-2}$ and Kr^{14+} , 280 keV, $5 \times 10^{15} \text{ cm}^{-2}$). It is shown, that irradiation causes compressive macrostress development, especially in regions of maximum damage dose and maximum implanted particles concentration. Also helium ion irradiation causes dislocation density increase in irradiated region, and krypton irradiation tends to decrease dislocation density in the area of maximum damage. As observed, more complex CoCrFeMnNi alloys is more resistant to defect formation than more simple CoCrFeNi.

Keywords: high-entropy alloys, ion irradiation, dislocations, macrostress, X-ray diffraction

1. Introduction

Modern challenges in the fields of nuclear energy are concentrated greatly across the increment of power and efficiency of nuclear facilities by increasing their working temperatures [1–3]. Classical materials, such as steels (including austenitic), nickel and other metal alloys with a binary base, are facing phase transformations and significant degradation of physical and mechanical properties at elevated temperatures, corroding when in contact with liquid coolants and some gases, and swelling under high doses of neutron irradiation [2, 3].

One of the most perspective classes of materials for the aims named upper can be high-entropy alloys (HEAs) [1–7]. They are new perspective class of materials, attracting the interest of the scientists from the whole world. The vanguard works on the theme of high-entropy alloys belong to Senkov and Kantor [8, 9].

It was found out that HEAs can have a structure, which differs from the structures of many homogeneous solid solutions: in some cases, they cannot be represented as a solid solution with a crystal lattice based on the lattice of one single element [1, 7]. Elevated entropy of mixing the constituent elements reduces the Gibbs free energy of the system and thus increases the thermodynamic stability of the HEA. Considering the variety of multicomponent solid solutions that are theoretically possible to be created, the nature may allow the creating of a HEAs with absolutely any properties [10, 11].

2. Experimental

2.1. Samples preparation and non-irradiated state

The samples of CoCrFeNi and CoCrFeMnNi high-entropy alloys were deposited by arc melting of pure metals (99.97%) powders in high-purity argon atmosphere. The ingots were annealed at 1150 °C for 24 h before cold rolling (85% thickness reduction) and for 72 h after it.

The X-ray diffraction phase analysis (Fig.1, Fig.2) showed the formation of a single-phase solid solution with FCC lattice for both CoCrFeNi and CoCrFeMnNi samples. The results of scanning electron microscopy and X-ray energy dispersive analysis confirm the formation of homogeneous near-equiautomatic multicomponent solid solutions, the grain size in the CoCrFeNi and CoCrFeMnNi alloys was about 80 and 100 μm , respectively.

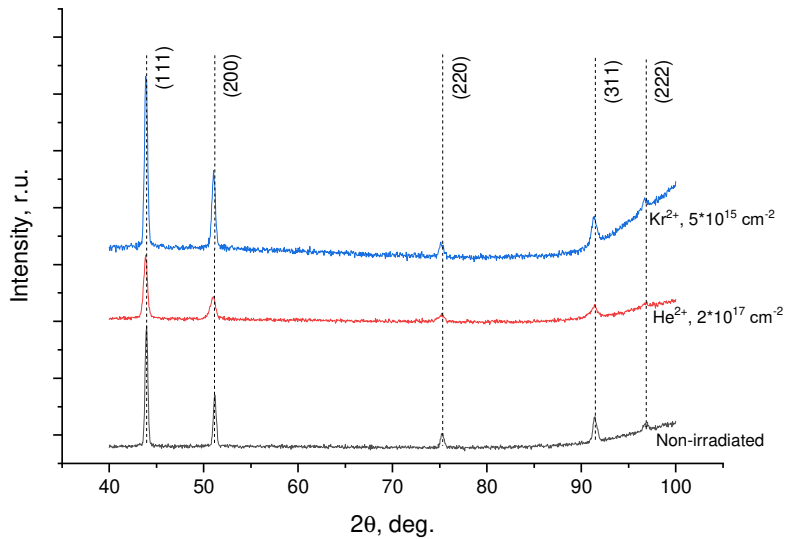


Fig.1. XRD spectra of CoCrFeNi samples: non-irradiated, after He and Kr ion irradiation.

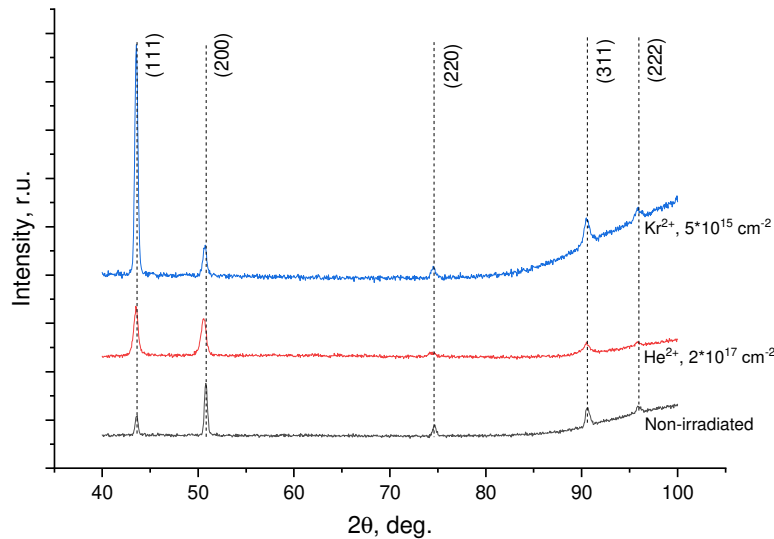


Fig.2. XRD spectra of CoCrFeMnNi samples: non-irradiated, after He and Kr ion irradiation.

X-ray studies of the distribution of internal macrostresses and dislocation density in the NiCoFeCr alloy irradiated with helium and krypton ions over depth were carried out using the $\sin^2\psi$ and Williamson-Hall methods, respectively.

It was revealed that internal macrostresses in non-irradiated CoCrFeNi and CoCrFeMnNi alloys are tensile and are about 125 and 68 MPa, respectively (Fig.3). They could be the consequences of cold rolling, causing the mechanical response of the system on compression.

2.2. Irradiated state and structural changes

It was found that irradiation with helium and krypton ions leads to the formation of compressive macrostresses without appearance of any additional diffraction reflexes that means phase composition stability of both HEAs. The stress level in samples irradiated with helium equals

-192 and -288 MPa for CoCrFeNi and CoCrFeMnNi alloys (Fig.3), respectively, also the shift of diffraction reflexes to the smaller diffraction angles observed (Fig.1, Fig.2), what tells about defect formation, causing the swelling of crystal grains. The stress level in samples irradiated with helium exceeds the values for samples irradiated with krypton ions (-6 and -17 MPa for CoCrFeNi and CoCrFeMnNi alloys, respectively, what is shown on Fig.3). Dislocation density in CoCrFeMnNi increases in both He and Kr irradiation because of defect formation and decreases in case of Kr irradiated CoCrFeMnNi because of greater chemical complexity (Fig.4).

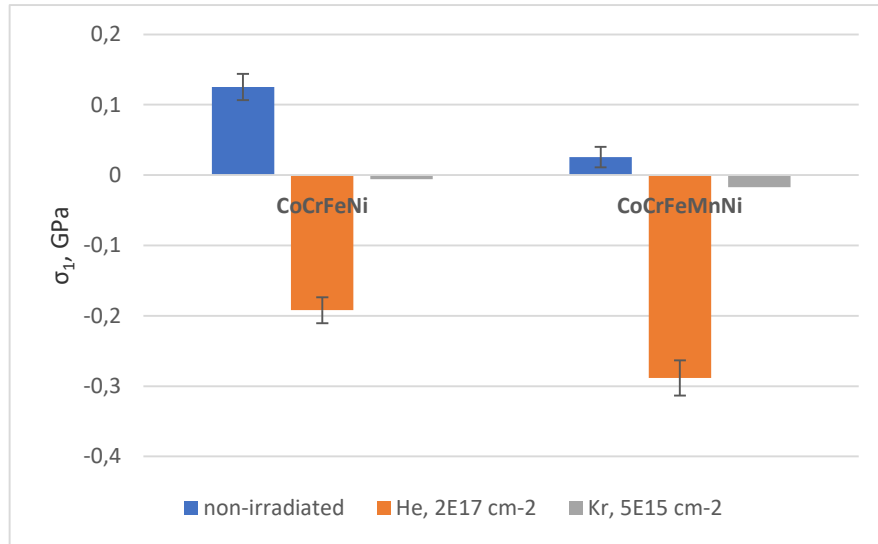


Fig. 3. Macrostress diagram of HEAs samples: non-irradiated, after He and Kr ion irradiation.

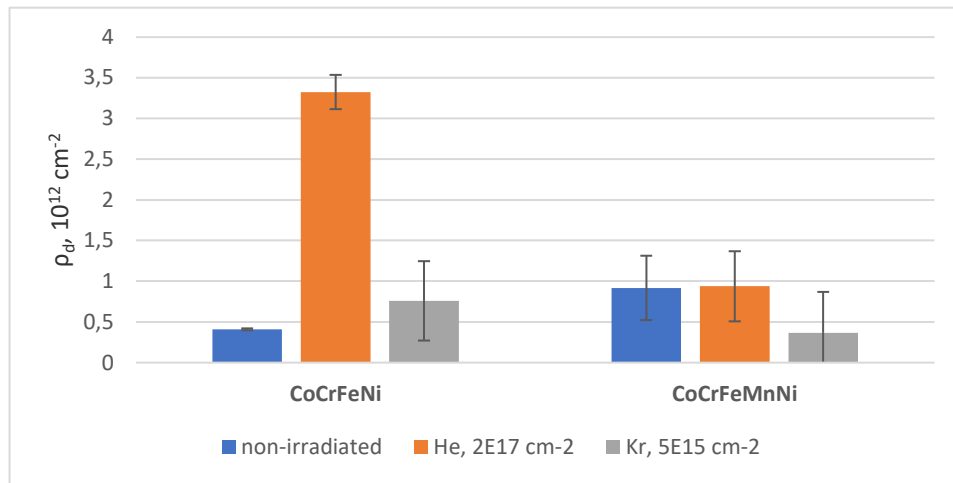


Fig. 4. Dislocation density diagram of HEAs samples: non-irradiated, after He and Kr irradiation.

It was found that the distribution of macrostress residual values in the CoCrFeNi alloy has two maxima corresponding to -250 MPa at a depth of 100 ± 25 nm and -530 MPa at a depth of 210 ± 25 nm (Fig.5). The results obtained are consistent with the SRIM data. According to calculations, the maximum radiation damage (dpa) corresponds to a depth of 125 nm, and the maximum of the implanted helium peak corresponds to a depth of 164 nm. The discrepancy in depth for the second maximum is mainly due to the swelling of the alloy during helium implantation.

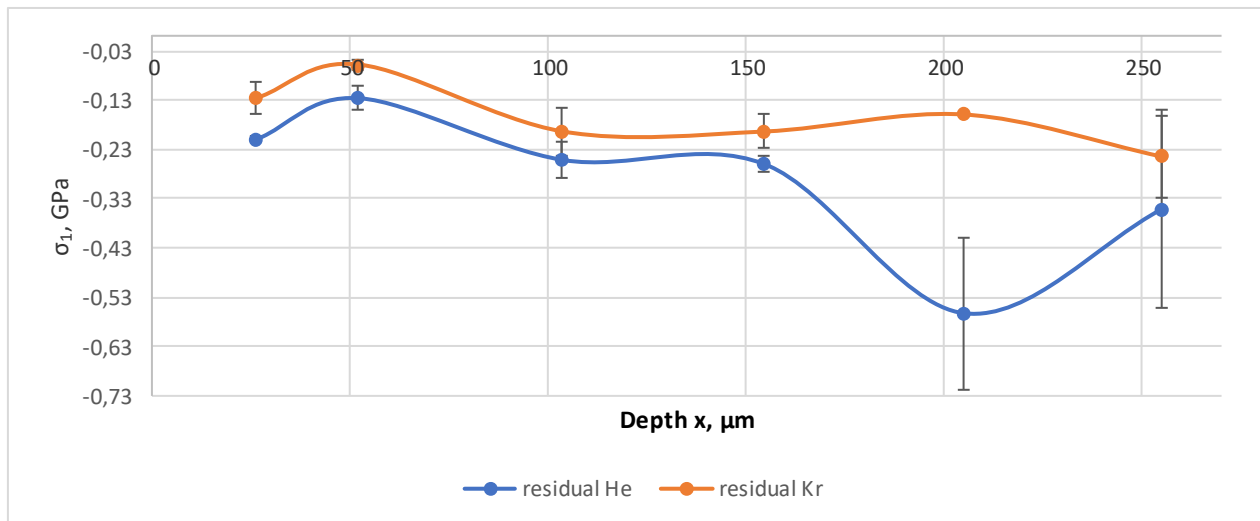


Fig.5. Macrostress change depth profile in CoCrFeNi after He and Kr ion irradiation.

It was found that the increase in the dislocation density in He-irradiated CoCrFeNi alloy compared to the non-irradiated alloy is $3.5 \times 10^{12} \text{ cm}^{-2}$ and remains constant in depth up to 150 nm, and then decreases to near-zero magnitudes (Fig.6). The region of dislocation density change is the same with irradiated region.

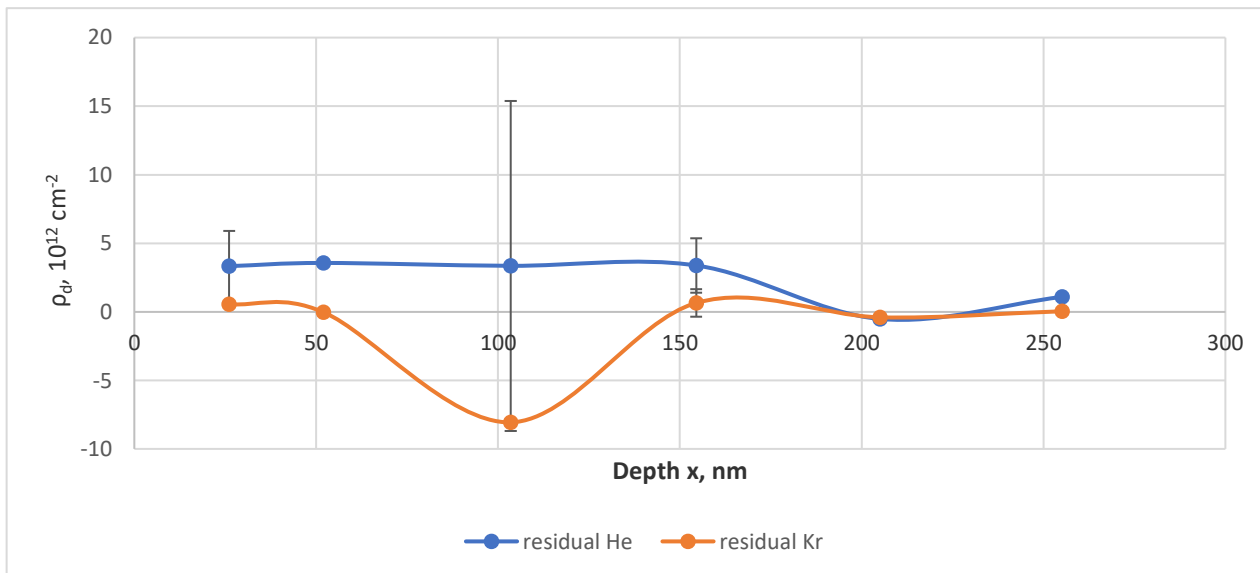


Fig.6. Dislocation density change depth profile in CoCrFeNi after He and Kr ion irradiation.

Comparing Kr-irradiated sample with non-irradiated, one can observe maximum of dislocation density decrease with $8.0 \times 10^{12} \text{ cm}^{-2}$ magnitude.

3. Discussion

3.1. Stress evolution

The mechanism of macrostress behavior seems to be in the radiation swelling of grains, which is the consequence of ion implantation and gas-vacancy complex aggregation and void formation. The increase of grain size and common swelling leads to compressive macrostress response. In case of He irradiation the pressure inside the gas bubbles and density of these bubbles are greater than in

case of Kr irradiation, as implanted He concentration is an order greater, than Kr. It results in greater compressive macrostress magnitude in case of He irradiated samples.

CoCrFeMnNi has greater compressive macrostresses than CoCrFeNi, because quinary alloy has more complex structure, which enhances diffusion suppression effect of high-entropy alloys and this way resists the aggregation of defects. Defects are unable to aggregate efficiently, which suppresses stress relaxation.

In He-irradiated CoCrFeNi the 210 ± 25 nm maximum on compressive macrostress depth profile corresponds to maximum bubble formation, which is shifted deeper from maximum of implanted He irradiation. The size of bubbles is great enough to cause compressive macrostress increase. In case of Kr-irradiated sample the absence of this maximum observed, while radiation damage maximum on depth of 100 ± 25 nm correlate with He-irradiated sample and is connected with dislocation dynamics.

3.2. Dislocation density evolution

As average dislocation density change in case of He-irradiated CoCrFeMnNi is lower than in CoCrFeNi, CoCrFeMnNi is more resistant to defect formation than CoCrFeNi. In CoCrFeNi dislocation density decreases after Kr irradiation on depth of 110 nm, which corresponds to maximum damage dose. Such effect can be achieved with vacancy formation, while dislocations mainly have interstitial nature. Together with diffusion suppression effect vacancies recombine on dislocations, decreasing their density and performing some kind of radiation annealing. After He irradiation of CoCrFeNi dislocation density increased on near-constant value in irradiated region, this situation can be explained by the interaction of dislocations with helium bubbles: bubbles can work as a sinks for vacancies and as barriers for dislocation migration, helping dislocations not to decrease their amount.

4. Conclusion

In this work non-irradiated, He- and Kr-irradiated bulk samples of high-entropy alloys CoCrFeNi and CoCrFeMnNi were examined with the help of X-ray diffraction analysis. Irradiation with He and Kr causes grain swelling and increase of compressive macrostresses in both materials, but He creates stable gas bubbles and voids due to high implanted particles concentration, while Kr creates mostly free vacancies and small density of bubbles, decreasing the dislocation density in irradiated region.

CoCrFeMnNi is more complex alloy than CoCrFeNi, which makes it to resistant to defect formation and aggregation. To build more accurate and veracious theoretical model transmission electron microscopy results are to be obtained for verifying the data.

Acknowledgement

This work was financially supported by State Program of scientific research “Energy and nuclear processes and technologies” (2.1.03.2). This research is funded by the Science Committee of the Ministry of Education and Science of the Republic of Kazakhstan (Grant No. AP14872199).

5. References

- [1] Ye Y.F., Wang Q., Lu J., Liu C.T., Yang Y., *Prog. Mat. Scien., Mater. Tod.*, 1, 2015; doi: 10.1016/j.mattod.2015.11.026
- [2] Manzoni A.M., Glatzel U., *Encyclopedia of Materials: Metals and Alloys*, 2020; doi: 10.1016/B978-0-12-803581-8.11774-6
- [3] Li W., Xie D., Li D., Zhang Y., Gao Y., Liaw P.K., *Progr. Mater. Scien.*, **118**, 100777, 2021; doi: 10.1016/j.pmatsci.2021.100777

-
- [4] Son S., Kim S., Kwak J., Gu G.H., Hwang D.S., Kim Y.T., Kim H.S., *Materials Letters*, **300**, 130130, 2021; doi: 10.1016/j.jmrt.2022.01.141
 - [5] Yu P.F., Zhang L.J., Cheng H., Zhang H., Ma M.Z., Li Y.C., Li G., Liaw P.K., Liu R.P., *Intermetallics*, **70**, 82, 2016; doi: 10.1016/j.intermet.2015.11.005
 - [6] Koval N.E., Juaristi J.I., Muiño R.D., Alducin M., *Journal of Applied Physics*, **127**, 145102, 2020; doi: 10.1063/1.5142239
 - [7] Zhang Y., Zuo T.T., Tang Z., Gao M.C., Dahmen K.A., Liaw P.K., Lu Z.P., *Progress in Materials Science*, **6**, 1, 2014; doi: 10.1016/j.pmatsci.2013.10.001.
 - [8] Cantor B., Chang I.T.H., Knight P., Vincent A.J.B., *Materials Science Eng.*, **375**, 213, 2004; doi: 10.1016/j.msea.2003.10.257
 - [9] Senkov O.N., Scott J.M., Senkova S.V., Miracle D.B., Woodward C.F., *Journal of Alloys and Compounds*, **509**, 6043, 2011; doi: 10.1016/j.jallcom.2011.02.171
 - [10] Karati A., Guruvidyathri K., Hariharan V.S., Murty B.S., *Scripta Materialia*, **162**, 465, 2019; doi: 10.1016/j.scriptamat.2018.12.017
 - [11] Pacheco V., et al., *Inorganic Chemistry*, **58**, 811, 2019; doi: 10.1021/acs.inorgchem.8b02957